Condensed Matter Physics, 2011, Vol. 14, No 3, 33002: 1–10
DOI: 10.5488/CMP.14.33002
http://www.icmp.lviv.ua/journal

On the molecular mechanism of surface charge amplification and related phenomena at aqueous polyelectrolyte-graphene interfaces*

A.A. Chialvo[1 †], J.M. Simonson[2]

[1] Chemical Sciences Division Geochemistry and Interfacial Sciences Group, Oak Ridge National Laboratory, Oak Ridge, TN 37831–6110, U.S.A.

[2] Neutron Scattering Sciences Division, Oak Ridge National Laboratory, Oak Ridge, TN 37831–6475, U.S.A.

Received April 11, 2011, in final form May, 18, 2011

In this communication we illustrate the occurrence of a recently reported new phenomenon of surface-charge amplification, SCA, (originally dubbed overcharging, OC), [Jimenez-Angeles F. and Lozada-Cassou M., J. Phys. Chem. B, 2004, **108**, 7286] by means of molecular dynamics simulation of aqueous electrolytes solutions involving multivalent cations in contact with charged graphene walls and the presence of short-chain lithium polystyrene sulfonates where the solvent water is described explicitly with a realistic molecular model. We show that the occurrence of SCA in these systems, in contrast to that observed in primitive models, involves neither contact co-adsorption of the negatively charged macroions nor divalent cations with a large size and charge asymmetry as required in the case of implicit solvents. In fact the SCA phenomenon hinges around the preferential adsorption of water (over the hydrated ions) with an average dipolar orientation such that the charges of the water's hydrogen and oxygen sites induce magnification rather than screening of the positive-charged graphene surface, within a limited range of surface-charge density.

Key words: *molecular simulation, solid-fluid interfaces, aqueous polyelectrolytes, surface charge amplification, charge inversion and reversal*

PACS: *07.05.Tp, 61.20.Ja, 82.35.Rs, 68.08.-p, 61.20.Ja*

1. Introduction

The conventional view on the behavior of electrolyte solutions in contact with a charged surface hinges around the concept of surface-charge screening by the ions in solution, which ultimately renders the entire system electroneutral (for a detail discussion on the surface-charge screening phenomenon the reader should refer to references [1–3]). This screening might take the form of adsorption, i.e., by alternating layers of opposite charged ions that gives rise to an oscillatory behavior for the total axial charge-density and represented by charge reversal (CR) followed by charge inversion (CI) phenomena. Note that for primitive models, such as the Poisson-Boltzmann (PB) description, this (apparent surface charge or local net charge density $\sigma(z)$, vide infra) profile is actually exponentially monotonous, and consequently, it never changes sign [2].

CR and CI phenomena are obviously the result of the stacking of alternately charged species that manifest as non-monotonous (oscillatory) profiles for the local electric field and potential i.e., they depend on ion-ion correlations or they are correlation-induced phenomena [3]) whose most obvious practical application is the layer-by-layer deposition of polyelectrolyte toward membrane formation [4].

Jimenez-Angeles and Lozada-Cassou [1] have recently reported a new phenomenon, dubbed overcharging, that occurs during the adsorption of macroions in solution onto planar charged-surfaces, i.e., when the macroions bring with them counterions to the surface that contribute to the

*The submitted manuscript has been authored by the contractor of the U.S. Government under contract No. DE–AC05–00OR22725. Accordingly, the U.S. Government retains a nonexclusive, royalty-free license to publish or reproduce the published form of this contribution, or allow others to do so, for U.S. Government purposes.

†E-mail: chialvoaa@ornl.gov, FAX 865-574-4961

© A.A. Chialvo, J.M. Simonson, 2011

buildup of a like charge. This phenomenon was initially revealed by integral equation calculations of three-component inhomogeneous primitive models of macroion solutions in contact with a positive-charged surface, and represented the adsorption of "an effective charge onto a like-charged" surface. In fact, when referring to this new phenomenon the authors indicated that "*such an effect defines a new phenomenon, hereafter referred to as overcharging (OC), i.e., at the wall's neighborhood we find the accumulation of an effective additional charge with the same sign of the wall. This effect is due to the strong electrostatic attraction between macroions and the divalent cations. However, for this effect to be present, a high particle's excluded volume is needed, i.e., a high concentration of macroions and/or little particles and/or large macroion size or little ion size*".

Other authors have reported OC phenomena since the original work of Jimenez-Angeles and Lozada-Cassou [1], involving either bulk [5, 6] or interfacial [7–9] macroion solutions. A common denominator in all these studies [1, 5–10] is the involvement of primitive models that ignore the discrete molecular-based nature of the solvent, and therefore, they neglect among other things the excluded volume of the solvent and the solvation effects that translate into significant dielectric inhomogeneous environments around the charged species.

The goal of this communication is to illustrate, by molecular dynamics simulation, the occurrence of OC in model aqueous electrolytes solutions involving multivalent cations in contact with positive-charged graphene walls in the presence of short-chains of lithium polystyrene sulfonate, where all species including the solvent water are explicitly and atomistically described. We argue that the occurrence of OC in these explicit solvent systems involves the preferential adsorption of the water's hydrogen and oxygen sites rather than the co-adsorption of the negative-charged macroions and the divalent cations with a large size and charge asymmetry, as observed in the primitive systems.

To address this issue, we perform extensive molecular dynamics simulations on similar systems to those described in our previous work [11], over a wider range of positive surface charges as described in section 2. In section 3 we present and discuss the relevant axial profiles to identify the molecular mechanism underlying the OC mechanism in these systems. Finally, in section 4 we discuss the contrasting differences between the OC phenomenon involving implicit and explicit description of the solvent water.

2. Fundamentals and simulation approach

The word "overcharging" has been most often used to describe the process of "overcompensation" of the surface charge on a solid substrate or a macroion due to the adsorption of multivalent counterions (e.g., references [12, 13]), a phenomenon that has been known for a rather long time under alternative names including "charge inversion" [13, 14], "charge overcompensation" [15], and "charge reversal" [16]. However, here we are dealing with a relatively new phenomenon, first reported by Jimenez-Angeles and Lozada-Cassou [1], involving the "amplification" of the surface charge, i.e., the actual increase of the original surface charge by the co-adsorption of macro- and micro-ions. In what follows we will invoke Jimenez-Angeles et al.'s definition of OC that describes the adsorption of an effective charge onto a like-charged wall (see also italicized quote vide supra), though we will rather refer to as the surface charge amplification (SCA) phenomenon [5, 7] to avoid any confusion with related phenomena, and illustrate how the differential hydration behavior of hydrated ions and polyions in conjunction with the significant graphene-water interactions contributes to its occurrence.

To study the SCA in the current systems we place emphasis on the determination of the axial distribution profiles that characterize the structure of the graphene-aqueous interface, including all species concentrations $\rho_i(z)$, the corresponding Coulombic charge density $\rho_Q(z)$, and the relative orientation of the water molecules $\theta(z)$ as follows [11],

$$\mathrm{P}(z) \equiv \left\langle (L_x L_y \Delta)^{-1} \sum_i \mathrm{P}_i \, \mathrm{B_c}\left(z_i\,, -0.5\Delta, +0.5\Delta\right) \right\rangle \tag{2.1}$$

for which P_i denotes $\delta(z - z_i)$, the Coulombic charge q_i, and the angle $\theta = \cos^{-1}\left(\boldsymbol{\mu}_\iota \cdot \hat{z}/\left|\boldsymbol{\mu}_\iota\right|\right)$

between the water's dipole moment $\boldsymbol{\mu}_i$ and the unit vector $\hat{z}$ perpendicular to the graphene surface, respectively, while $\mathrm{B_c}(x,a,b) \equiv [\Theta(x-a) - \Theta(x-b)]$ defines the "boxcar" function [17], L_α represents the size of the simulation box along the α-axis, $\Delta \sim 0.3$ Å, and the $\langle \cdots \rangle$ indicates a time average over the simulation trajectory. Note that the first two distributions are connected by the expression $\rho_Q(z) = \sum_i x_i q_i \rho_i(z)$, the one that we use for a test of internal consistency.

Subsequently, the axial integration of $\rho_Q(z)$ according to the Poisson equation provides us with a way to assess the strength of the (normalized) surface-charge screening, $\mathfrak{I}(z) \equiv 1 - (\sigma(z)/\sigma_\mathrm{s})$, where the local net (surface) charge density $\sigma(z)$ is given by,

$$\sigma(z) = \sigma_\mathrm{s} + \int_0^z \rho_Q(z)\,\mathrm{d}z \tag{2.2}$$

subjected to the electroneutrality condition $\sigma(h) = 0$, i.e.,

$$\sigma_\mathrm{s} = -\int_0^h \rho_Q(z)\,\mathrm{d}z. \tag{2.3}$$

Consequently, according to Gauss' law, the profile of the electric field $E(z)$ corresponding to $\sigma(z)$ becomes,

$$E(z) = 4\pi\sigma(z) \tag{2.4}$$

with $E(0) = 4\pi\sigma(0)$, i.e., $\sigma(0) = \sigma_\mathrm{s}$, and from equations (2.2)–(2.4) it follows that,

$$E(z) = -4\pi \int_z^h \rho_Q(z)\mathrm{d}z. \tag{2.5}$$

Now, we can reinterpret the strength of the surface-charge screening $\mathfrak{I}(z)$ as follows,

$$\mathfrak{I}(z) = 1 - [E(z)/E(0)] \tag{2.6}$$

where equation (2.6) describes how effectively the aqueous electrolyte-polyelectrolyte screens the surface charge of the graphene wall. While $\mathfrak{I}(z)$ satisfies two obvious conditions, i.e., null screening, $\mathfrak{I}(0) = 0$, and full screening, $\mathfrak{I}(h) = 1$, this function might not be necessarily bounded by those conditions due to the non-monotonous behavior of $\rho_Q(z)$. It is quite possible to find (vide infra) that the most interesting interfacial phenomena involving adsorption of macroions in the presence of aqueous electrolytes are associated with the condition $0 > \mathfrak{I}(z) > 1$.

In principle, the integrated fluid charge $\sigma(z) - \sigma_\mathrm{s} = \int_0^z \rho_Q(z)\mathrm{d}z$ can exhibit an oscillatory behavior around electroneutrality, yet, for a positive-charged surface ($\sigma_\mathrm{s} > 0$) the graphene-aqueous electrolyte interface would display three distinct types of behavior, depending on the strength of the local net (surface) charge density at its first extreme (peak or valley), i.e., $\sigma(z_\otimes) = \sigma_\otimes$, relative to the surface charge σ_s , namely:

(a) surface-charge amplification (SCA), i.e.,

$$\sigma_\otimes > \sigma_\mathrm{s} > 0 \quad \rightarrow \quad \int_0^{z_\otimes} \rho_Q(z)\mathrm{d}z > 0 \quad \rightarrow \quad \mathfrak{I}(z_\otimes) < 0; \tag{2.7}$$

(b) charge inversion (CI), i.e.,

$$\sigma_\mathrm{s} > \sigma_\otimes > 0 \quad \rightarrow \quad \sigma_\mathrm{s} > -\int_0^{z_\otimes} \rho_Q(z)\mathrm{d}z \quad \rightarrow \quad \mathfrak{I}(z_\otimes) < 1; \tag{2.8}$$

(c) charge reversal (CR), i.e.,

$$\sigma_{\otimes} < 0 \quad \rightarrow \quad \sigma_{\rm s} < -\int\limits_{0}^{z_{\otimes}} \rho_{Q}(z)\mathrm{d}z \quad \rightarrow \quad \mathfrak{I}(z_{\otimes}) > 1. \tag{2.9}$$

Our systems comprised aqueous electrolyte solutions involving short-chain lithium polystyrene-sulfonate in contact with a positive-charged graphene surface, $0 \leqslant \sigma_{\rm s}(\mathrm{C\ m^{-2}}) \leqslant 0.1525$, with added barium chloride to render the systems electroneutral. Full details of the simulation methodology, description of the models, system sizes and relevant simulation parameters are given in our previous work [11], consequently, here we only provide the most relevant information regarding the system composition and surface charge in table 1.

Table 1. Surface charge and composition of aqueous polyelectrolyte solutions.

System	$\sigma_{\rm s}$/C m^{-2}	$q_{\rm s}{}^{(a)}$	$N_{\rm Li^+}$	$N_{\rm Ba^{2+}}$	$N_{\rm Cl^-}$	$N_{\rm H_2O}$	$N_{\rm SO_3^-}$
1	0.1525	30	100	20	90	4000	80
2	0.1017	20	100	20	80	4000	80
3	0.0763	15	100	20	75	4000	80
4	0.0508	10	100	20	70	4000	80
6	0.0254	5	100	20	65	4000	80
7	0	0	100	20	60	4000	80
$8^{(b)}$	0	0	0	0	0	4000	0

$^{(a)}$Total electrostatic charge at carbon sites exposed to the fluid phase.
$^{(b)}$Pure water in contact with the graphene wall.

3. Discussion of simulation results

In figure 1 we display the axial profiles for the average charge densities, corresponding to the surface-charge range of $0 \leqslant \sigma_{\rm s}(\mathrm{C\ m^{-2}}) \leqslant 0.1525$, within the first 12 Å from the graphene surface, in comparison with that corresponding to pure water in contact with the uncharged graphene surface. The first relevant feature in this comparison is the appearance of an additional peak about 3.5–4 Å from the graphene surface, sandwiched between the original two in the pure-water profile, originated in the adsorption of hydrated charged species (including paired and condensed cations). In addition, there is a strong reduction of the size of the first peak of the charge density (located at ~ 2.6 Å) with a simultaneous strengthening of the second peak (at ~ 3.5–4 Å) as the surface-charge increases to the extent that the first peak disappears as the surface charge approaches $\sigma_{\rm s} \cong 0.1525\ \mathrm{C\ m^{-2}}$. The observed decrease of the strength of the first peak is accompanied by an increase of the strength of the second peak and the deepening of the two corresponding valleys (at ~ 3 Å and ~ 4.5 Å), a behavior that points to the re-structuring of the interfacial region through the adjustment of species adsorption and water re-orientation as we illustrate below. In fact, figure 2 captures the evolution of the relative dipolar orientation of the water molecules in the interfacial region, where it becomes clear that the hydrogen sites of the water molecules in the adsorbed layer of either a graphene/water or graphene/aqueous interface with $\sigma_{\rm s} = 0$ are tilted toward the graphene surface, i.e., $\theta > 90^{\circ}$. As we increase the surface charge, i.e., $\sigma_{\rm s} \rightarrow 0.1525\ \mathrm{C\ m^{-2}}$, the positive-charged hydrogen sites are repelled by the graphene charged surface, and consequently, $\theta \ll 90^{\circ}$.

The re-structuring of the interfacial region can be interpreted in terms of the axial profiles of the corresponding electric fields, $E(z)$, as illustrated in figure 3 where we should note that $\sigma_{\rm s} = E(0)/4\pi$ is represented by the horizontal lines ($z < 2.6$ Å), and that $0 \cong [\sigma(z_{\otimes}) - \sigma_{\rm s}] \lesssim 1.52$ where $2.6\ \text{Å} \lesssim z_{\otimes} \lesssim 2.92\ \text{Å}$ when $0 \leqslant \sigma_{\rm s}(\mathrm{C\ m^{-2}}) \leqslant 0.1525$. In this figure we again observe

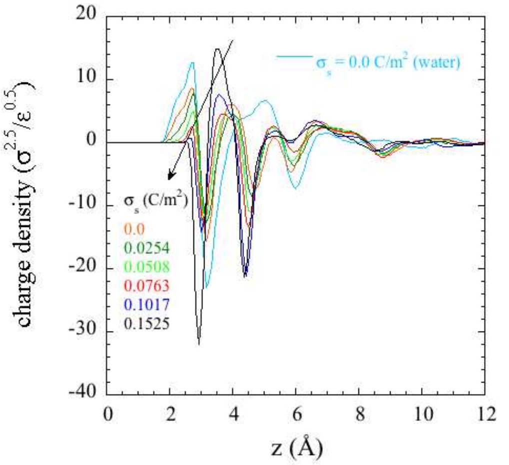

Figure 1. (Color on-line) Behavior of the axial profiles for the charge density, $\rho_Q(z)$, for the graphene/fluid interface when the fluid is either pure water at zero surface charge or an electrolyte-polyelectrolyte solution with a surface-charge range of $0 \leqslant \sigma_s(\mathrm{C\ m^{-2}}) \leqslant 0.1525$. Charge densities in units of SPC/E Lennard-Jones parameters $\sigma_{OO} = 3.166$ Å and $\varepsilon_{OO}/k = 78.23$ K.

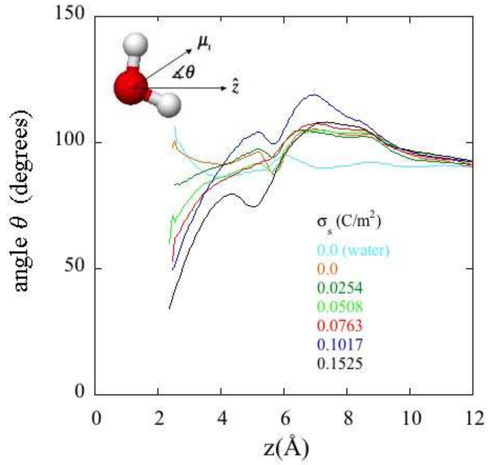

Figure 2. (Color on-line) Behavior of the axial profiles for the relative orientation $\theta(z)$ of the water molecules in the graphene/fluid interface when the fluid is either pure water at zero surface charge or an electrolyte-polyelectrolyte solution with a surface-charge range of $0 < \sigma_s(\mathrm{C\ m^{-2}}) \leqslant 0.1525$.

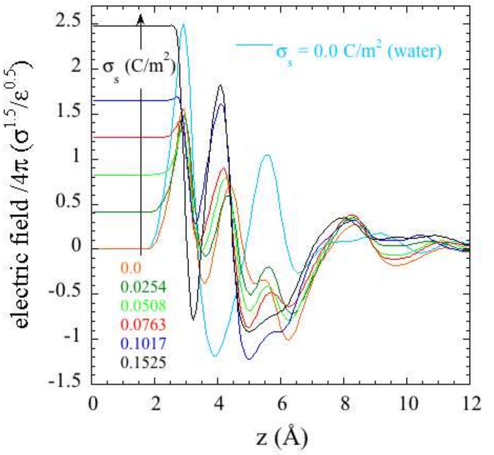

Figure 3. (Color on-line) Behavior of the axial profiles for the integrated fluid charge density, $\sigma(z) = E(z)/4\pi$, for the graphene/fluid interface when the fluid is either pure water at zero surface charge or an electrolyte-polyelectrolyte solution with a surface-charge range of $0 \leqslant \sigma_s(\mathrm{C\ m^{-2}}) \leqslant 0.1525$. Integrated charge densities in units of SPC/E Lennard-Jones parameters $\sigma_{OO} = 3.166$ Å and $\varepsilon_{OO}/k = 78.23$ K.

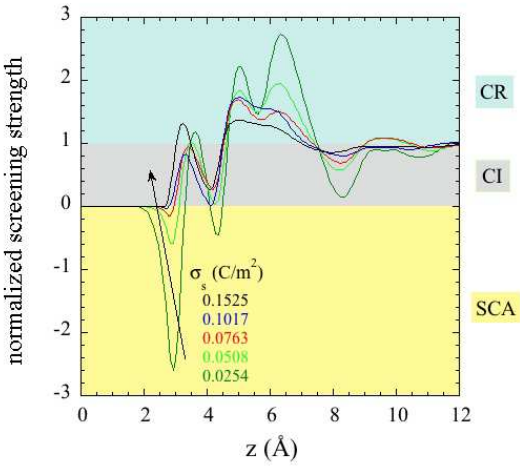

Figure 4. (Color on-line) Behavior of the axial profiles for the normalized screening strength axial profiles, $\mathfrak{J}(z) \equiv 1 - (\sigma(z)/\sigma_s)$, for the graphene/fluid interface when the fluid is either pure water at zero surface charge or an electrolyte-polyelectrolyte solution with a surface-charge range of $0 < \sigma_s(\mathrm{C\ m^{-2}}) \leqslant 0.1525$.

the appearance of a third peak at $\sim$ 4–4.5 Å from the graphene surface, which moves closer to the surface as the graphene surface-charge increases in response to the stronger wall-polyion interactions and the related counterion condensation. However, the most revealing feature in this plot is the size of the electric field "barrier" $[E(z_{\otimes}) - E(0)]_{\sigma_{\mathrm{s}}}$ represented by the first peak of $E(z)$ that signifies the occurrence of the SCA phenomenon. Interestingly, the oscillatory behavior of $E(z)$ translates into an SCA phenomenon even for the case of an uncharged surface, $\sigma_{\mathrm{s}} = 0$, for which the electric field "barrier" $[E(z_{\otimes}) - E(0)]_{\sigma_{\mathrm{s}}=0}$ takes the largest value. Yet, a more revealing way to look at the SCA and related phenomena is by plotting the normalized screening strength $\mathfrak{J}(z)$ in figure 4, and observe the three distinct regions described by equations (2.7)–(2.9). Note that the SCA signature in our system is revealed by the prominent first valley $\mathfrak{J}(z_{\otimes}) < 0$ that disappears as $\sigma_{\mathrm{s}} \to 0.1525$ C m^{-2}.

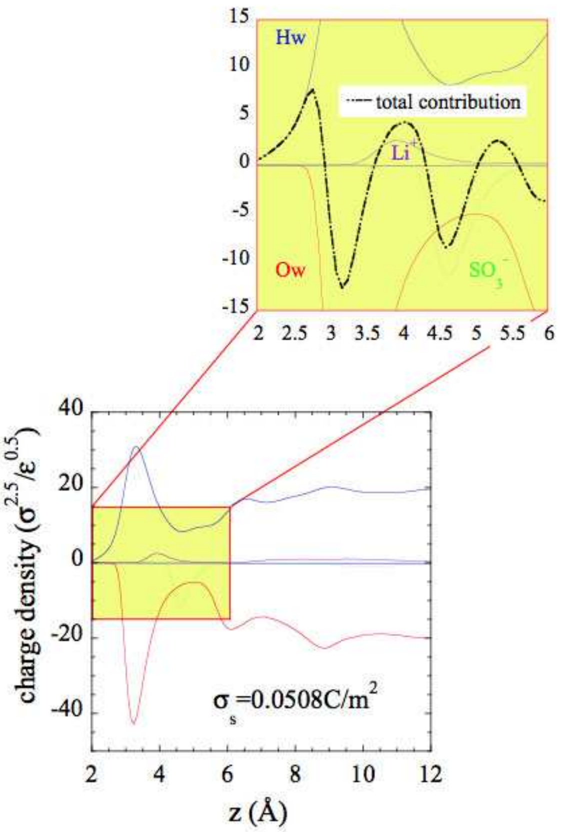

Figure 5. (Color on-line) Individual species contributions, $q_i\rho_i(z)$, to the axial profiles of the charge density, $\rho_Q(z)$, for the graphene/fluid interface when the fluid is an electrolyte-polyelectrolyte solution with a surface-charge of $\sigma_{\mathrm{s}} = 0.0508$ C m^{-2}.

The results in figures 1–4 suggest that the observed SCA must be associated with the competing adsorption of water, hydrated ions and poly-ions onto the graphene layer. This competition is obviously absent in the case of primitive models where the continuum solvent plays the passive role of a dielectric screener of the electrostatic interactions, i.e., there is no inhomogeneous interfacial solvent distribution due to its interaction with the solid phase. In order to shed additional light onto the SCA mechanism, and concomitant CR and CI, in figure 5 we plot the individual contribution of each charged site to the charge-density profile for the representative surface-charge $\sigma_{\mathrm{s}} = 0.0508$ C m^{-2}. From the zoomed in portion of this picture it becomes clear that the oxygen and hydrogen sites of the first layer of adsorbed water are the sole contributors to the first peak and valley of the charge-density profile, and consequently, to the SCA peak in figure 3. Note also that the hydrated lithium ion makes an additional positive contribution to the second peak of the charge-density profile $\rho_Q(z)$, whose main contribution comes from the balance between the oxygen and hydrogen sites of the innermost (adsorbed) water layer. Moreover, while the sulfonate groups from the innermost PE backbones make the main contribution to the second valley of $\rho_Q(z)$, a balance between the charged sites of water and the sulfonate groups define almost exclusively the third peak.

4. Concluding remarks

We have performed a molecular dynamics simulation study of the interfacial behavior of short-chain lithium polystyrene-sulfonate aqueous solutions in contact with positive-charged graphene surfaces, in the presence of barium chloride, to highlight the central role that the discrete nature of the solvent plays in the occurrence of surface charge amplification. In contrast to other recent studies [5–10, 18], here we have used explicit and realistic descriptions of the solvent water, the chain backbones, and the ionic species in solution that allowed us to unravel the mechanism underlying the screening of the surface charge by the surrounding aqueous environment.

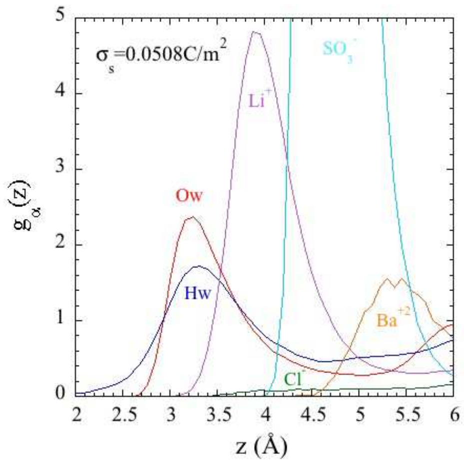

Figure 6. (Color on-line) Individual species axial distribution functions, $g_i(z) = \rho_i(z)/\rho_i^{\mathrm{bulk}}$, for the graphene/fluid interface when the fluid is an electrolyte-polyelectrolyte solution with a surface-charge of $\sigma_{\mathrm{s}} = 0.0508$ C m^{-2}.

In particular, the simulated interfacial structures indicate that the SCA resulting from the adsorption of short-chain polystyrene-sulfonates onto charged surfaces originates in the induced orientational structure of the interfacial water, where the water's hydrogens and oxygens lay in parallel planes with opposite density charges, aided by the adsorbed polyelectrolyte chains and condensed counterions, though contributing only marginally by enforcing the system electroneutrality. Consequently, the magnitude of the SCA depends mainly on the relative overlapping of the distribution of the hydrogen- and oxygen-site charges (see figure 6), which in turn, is controlled by the tilt angle $\theta(z)$ (figure 2). In other words, the solvent (water), rather than the ionic species, becomes the major player in the SCA phenomenon; water mediates the interactions of all species with the charged surface, i.e., the ions are adsorbed as hydrated species. This scenario highly contrasts with that from SCA phenomena observed by theory [1, 5, 6] and simulation [8, 9, 18, 19] involving primitive models, where a continuum dielectric describes the solvent in the screening of the Coulombic interactions. Yet, we can draw some common features between the two scenarios by recognizing that when the solvent water is described atomistically as an electroneutral set of bonded charged-sites, it plays the same role as any charged species in the system, except for its ability to solvate the species due to its polar nature that hinders other species from approaching the surface. Consequently, while our analysis suggests an SCA mechanism similar to that proposed originally by Jimenez-Angeles and Lozada-Cassou [1] (e.g., see insets of their figure 2), we must highlight some significant conceptual differences with the latter, namely: (a) the magnitude and asymmetry of the charges involved in our system are much smaller, i.e., $q_{\mathrm{H_w}} = 0.4238e = -0.5q_{\mathrm{O_w}}$ in comparison to $q_{\mathrm{M}} = -40e = -20q_+ = 40q_-$ in reference [1], resulting in a charge asymmetry of 2 compared to 20 in reference [1], and (b) in our case the partial charges on the sites of the electroneutral polar solvent are linked by the intramolecular $\mathrm{O-H}$ bonds, i.e., they are correlated by construction.

While we have tackled the specific case of SCA when $\sigma_{\mathrm{s}} > 0$, a similar phenomenon can in principle happen for $\sigma_{\mathrm{s}} < 0$ (e.g., see figure 4 (c)–(d) of Wang et al. [8], and figure 4 (b) of Tanaka and Grosberg [19] which was not recognized as such until recently [7]). Following a similar analysis as for equations (2.7)–(2.9), their counterparts for the case of $\sigma_{\mathrm{s}} < 0$ become,

(a) surface-charge amplification (SCA), i.e.,

$$|\sigma_\otimes| > |\sigma_{\mathrm{s}}| > 0 \quad \rightarrow \quad \int_0^{z_\otimes} \rho_Q(z)\mathrm{d}z < 0 \quad \rightarrow \mathfrak{J}(z_\otimes) < 0; \tag{4.1}$$

(b) charge inversion (CI), i.e.,

$$|\sigma_{\mathrm{s}}| > |\sigma_\otimes| > 0 \quad \rightarrow \quad |\sigma_{\mathrm{s}}| > \int_0^{z_\otimes} \rho_Q(z)\mathrm{d}z \quad \rightarrow \mathfrak{J}(z_\otimes) < 1; \tag{4.2}$$

(c) charge reversal (CR), i.e.,

$$\sigma_{\otimes} > 0 \quad \to \quad |\sigma_{\mathrm{s}}| < \int_{0}^{z_{\otimes}} \rho_Q(z)\mathrm{d}z \quad \to \ \mathfrak{I}(z_{\otimes}) > 1. \tag{4.3}$$

Thus, according to equations (2.7)–(2.9) and (4.1)–(4.3), the general conditions for the occurrence of SCA, CI and CR for an arbitrary surface charge $\sigma_{\mathrm{s}} \gtrless 0$ can be described as follows,

$$(\sigma_{\otimes}\sigma_{\mathrm{s}}) > 0 \quad \text{with}\, |\sigma_{\otimes}| > |\sigma_{\mathrm{s}}| \quad \to \mathrm{SCA}, \tag{4.4}$$
$$(\sigma_{\otimes}\sigma_{\mathrm{s}}) > 0 \quad \text{with}\, |\sigma_{\otimes}| < |\sigma_{\mathrm{s}}| \quad \to \mathrm{CI}, \tag{4.5}$$
$$(\sigma_{\otimes}\sigma_{\mathrm{s}}) < 0 \quad \text{with}\, |\sigma_{\otimes}| \gtrless |\sigma_{\mathrm{s}}| \quad \to \mathrm{CR}. \tag{4.6}$$

We should mention that Tanaka and Grosberg [19] analyzed the ion adsorption/condensation onto macroion surfaces by molecular dynamics of primitive models and described the over-screening of the negative-charged macroion as a "giant charge inversion". In particular, we note that their figure 2 dealing with a $Q(r \approx 3a)/\,|Q_0| \approx 2.5$ and $Q_0 = -28e$ does not portray a CI as claimed but a CR phenomenon, i.e., $-Q(r \approx 3a)/Q_0 \sim \mathfrak{I}(3a) > 1$ according to equation (4.3), where the same conclusion can be reached by Guerrero-Garcia et al.'s [5] analysis involving their equation (5). Likewise, the behavior described in Tanaka and Grosberg's figure 4 (b) for $Q(r \approx 8a)/\,|Q_0| \approx -0.6$ and $Q_0 = -28e$ does not describe a CI but an SCA phenomenon because $-Q(r \approx 8a)/Q_0 \sim \mathfrak{I}(8a) < 0$ according to equation (4.3) and in agreement with Guerrero-Garcia et al.'s analysis [5].

Our analysis should be put in the context of, and in contrast against, the recent developments dealing mainly with primitive models. Since we are dealing with an explicit atomistic description of the solvent, our results point immediately to some yet unexplored issues including, (a) the potential effect of the water's flexible geometry on the strength of its adsorption on the grapheme surface and on the resulting charge screening, (b) the effect of confinement as a result of the overlapping of two approaching aqueous-graphene interfaces, and (c) the existence of a similar mechanism for the negative SCA involving the corresponding poly-cation species. Note that the proposed SCA mechanism is in principle independent of the involved water model, though the strength (and width of the surface-charge window in which SCA occurs) might depend on the water model chosen. In particular, we should expect a clear model dependence when comparing the simulation results from a rigid against its flexible geometry counterpart.

Acknowledgements

Research sponsored by the Division of Chemical Sciences, Geosciences, and Biosciences, Office of Basic Energy Sciences, U.S. Department of Energy.

References

1. Jimenez-Angeles F. and Lozada-Cassou M., J. Phys. Chem. B, 2004, **108**, No. 22, 7286; doi:10.1021/jp036464b.
2. Sjostrom L., Akesson T., and Jonsson B., Ber. Bunsen Ges. Phys. Chem., 1996, **100**, No. 6, 889; doi:10.1002/bbpc.19961000634.
3. Hansen J.P. and Lowen H., Annu. Rev. Phys. Chem., 2000, **51**, 209; doi:10.1146/annurev.physchem.51.1.209.
4. Decher G. and Hong J.D., Makromol. Chem. Macromol. Symp., 1991, **46**, 321; doi:10.1002/masy.19910460145; Dan N., Nano Lett., 2003, **3**, No. 6, 823; doi:10.1021/nl034122b; Pittler J., Bu W., Vaknin D., Travesset A., McGillivray D.J., and Loesche M., Phys. Rev. Lett., 2006, **97**, No. 4, 046102; doi:10.1103/PhysRevLett.97.046102.
5. Guerrero-Garcia G.I., Gonzalez-Tovar E., and de la Cruz M.O., Soft Matter, 2010, **6**, No. 9, 2056; doi:10.1039/B924438G.
6. Guerrero-Garcia G.I., Gonzalez-Tovar E., Chavez-Paez M., and Lozada-Cassou M., J. Chem. Phys., 2010, **132**, No. 5, 054903; doi:10.1063/1.3294555.
7. Messina R., J. Chem. Phys., 2007, **127**, No. 21, 214901; doi:10.1063/1.2807228.
8. Wang Z.-Y. and Ma Y.-Q., J. Phys. Chem. B, 2010, **114**, No. 42, 13386; doi:10.1021/jp106118q.
9. Wang Z.-Y. and Ma Y.-Q., J. Chem. Phys., 2010, **133**, No. 6, 064704; doi:10.1063/1.3469795.
10. Yu J., Aguilar-Pineda G.E., Antillon A., Dong S.H., and Lozada-Cassou M., J. Colloid Interface Sci., 2006, **295**, No. 1, 124; doi:10.1016/j.jcis.2005.08.016.
11. Chialvo A.A. and Simonson J.M., J. Phys. Chem. C., 2008, **112**, No. 49, 19521; doi:10.1021/jp8041846.
12. Gossl I., Shu L.J., Schluter A.D., and Rabe J.P., J. Am. Chem. Soc., 2002, **124**, No. 24, 6860; doi:10.1021/ja017828l; Maiti P.K. and Bagchi B., Nano Lett., 2006, **6**, No. 11, 2478; doi:10.1021/nl061609m; Lyulin S., Darinskii A., and Lyulin A., e-Polym., 2007, No. 097-1/14; Gillies G., Lin W., and Borkovec M., J. Phys. Chem. B, 2007, **111**, No. 29, 8626; doi:10.1021/jp069009z; Kundagrami A. and Muthukumar M., J. Chem. Phys., 2008, **128**, No. 24, 244901; doi:10.1063/1.2940199; May S., Iglic A., Rescic J., Maset S., and Bohinc K., J. Phys. Chem. B, 2008, **112**, No. 6, 1685; doi:10.1021/jp073355e.
13. Grosberg A.Y., Nguyen T.T., and Shklovskii B.I., Rev. Mod. Phys., 2002, **74**, No. 2, 329; doi:10.1103/RevModPhys.74.329.
14. Joanny J.F., Eur. Phys. J. B, 1999, **9**, No. 1, 117; doi:10.1007/s100510050747.
15. Dobrynin A.V., Deshkovski A., and Rubinstein M., Macromolecules, 2001, **34**, No. 10, 3421; doi:10.1021/ma0013713.
16. Diehl A. and Levin Y., J. Chem. Phys., 2006, **125**, No. 5, 054902; doi:10.1063/1.2222372; Pianegonda S., Barbosa M.C., and Levin Y., Europhys. Lett., 2005, **71**, No. 5, 831; doi:10.1209/epl/i2005-10150-y.
17. von Seggern D., Standard Curves and Surfaces. CRC Press, Boca Raton, 1993.
18. Ravindran S. and Wu J.Z., Langmuir, 2004, **20**, No. 17, 7333; doi:10.1021/la0493619; Messina R., Holm C., and Kremer K., Langmuir, 2003, **19**, No. 10, 4473; doi:10.1021/la026988n.
19. Tanaka M. and Grosberg A.Y., J. Chem. Phys., 2001, **115**, No. 1, 567; doi:10.1063/1.1377033.

Молекулярний механізм збільшення поверхневого заряду і споріднені явища на межі розділу водний поліелектроліт-графен

А.А. Кіалво[1], Дж.М. Сімонсон[2]

[1] Відділ хімічних наук, Національна лабораторія Оук Рідж, Оук Рідж, Тенессі, США
[2] Відділ досліджень нейтронним розсіянням, Національна лабораторія Оук Рідж, Оук Рідж, Тенессі, США

У статті нами розглянуто недавно виявлене явище збільшення поверхневого заряду (ЗПЗ) [Jimenez-Angeles F. and Lozada-Cassou M., J. Phys. Chem. B, 2004, **108**, 7286]. Методом молекулярної динаміки проведено моделювання водних розчинів електролітів з багатовалентними катіонами, що перебувають у контакті з графеновими стінками; воду в моделюванні представлено явно з використанням реалістичної молекулярної моделі. Нами показано, що явище ЗПЗ в таких системах, на відміну від примітивних моделей, не включає ні контактної коадсорбції негативно заряджених макроіонів, ні двовалентних катіонів з великою асиметрією у розмірах та зарядах, як це вимагається у випадку моделей з розчинниками, представленими як суцільне середовище. Насправді ефект ЗПЗ проявляється за рахунок вибіркової адсорбції води (через гідратовані іони) з напрямком диполів, орієнтованих таким чином, щоб підсилювати, а не екранувати позитивно заряджену поверхню графену.

Ключові слова: *молекулярне моделювання, межа розділу рідина-тверде тіло, водні полielектроліти, збільшення поверхневого заряду, зарядова інверсія і реверсування*